remote sensing

MDPI

Article

Influence of Climate, Topography, and Hydrology on Vegetation Distribution Patterns—Oasis in the Taklamakan Desert Hinterland

Lei Peng, Yanbo Wan, Haobo Shi, Abudureyimu Anwaier and Qingdong Shi *

College of Ecology and Environment, Xinjiang University, Urumqi 830046, China; penglei1028@stu.xju.edu.cn (L.P.); wanyb1995@stu.xju.edu.cn (Y.W.); shi_haobo@stu.xju.edu.cn (H.S.); anwar_jan@stu.xju.edu.cn (A.A.)
* Correspondence: shiqd@xju.edu.cn

Abstract: Vegetation in natural desert hinterland oases is an important component of terrestrial ecosystems. Determining how desert vegetation responds to natural variability is critical for a better understanding of desertification processes and their future development. The aim of this study is to characterize the spatial distribution of vegetation in the natural desert hinterland and to reveal how different environmental factors affect vegetation changes. Taking a Taklamakan Desert hinterland oasis as our research object, we analyzed the effects of different environmental factors on desert vegetation using a time-series normalized difference vegetation index (NDVI) combined with meteorological, topographic, and hydrological data, including surface water and groundwater data. Vegetation was distributed in areas with high surface water frequency, shallow groundwater levels, relatively flat terrain, and dune basins. NDVI datasets show greening trends in oasis areas over the past 20 years. The frequency of surface water distribution influences water accessibility and effectiveness and shapes topography, thus affecting the spatial distribution pattern of vegetation. In this study, areas of high surface water frequency corresponded with vegetation distribution. The spatial distribution of groundwater depth supports the growth and development of vegetation, impacting the pattern of vegetation growth conditions. Vegetation is most widely distributed in areas where the groundwater burial depth is 3.5–4.5 m. This study provides data for restoring riparian vegetation, ecological water transfer, and sustainable development.

Keywords: Taklamakan Desert hinterland; climate change; topography; hydrological processes; vegetation pattern

Citation: Peng, L.; Wan, Y.; Shi, H.; Anwaier, A.; Shi, Q. Influence of Climate, Topography, and Hydrology on Vegetation Distribution Patterns—Oasis in the Taklamakan Desert Hinterland. *Remote Sens.* **2023**, *15*, 5299. https://doi.org/10.3390/rs15225299

Academic Editor: Markus Immitzer

Received: 28 September 2023
Revised: 26 October 2023
Accepted: 7 November 2023
Published: 9 November 2023

1. Introduction

Vegetation is an important component of terrestrial ecosystems with a critical role in maintaining the sustainable development of global and regional ecosystems [1]. Desert vegetation supports the survival and development of oases. While vegetation in desert areas is typically sparse, it is instrumental in anchoring sand dunes and countering desertification [2]. Understanding how desert vegetation adapts to shifts in natural and human-induced stressors is crucial for a deeper comprehension of desertification dynamics and its prospective progression.

According to the fifth report from the Intergovernmental Panel on Climate Change (IPCC), global climate change has significantly intensified in recent years. In fact, the last 30 years have seen the highest average temperatures since 1400; meanwhile, rainfall has increased in humid zones and decreased in arid zones, with the frequency of extreme rainfall increasing [3]. These notable changes in climate impact the vegetation growth environment, which in turn affects the phenology, distribution, and growth of vegetation, thus affecting the ecosystem material–energy conversion and carbon cycle [4,5]. Climate influences the long-term evolution of vegetation and causes changes in vegetation growing

seasons by altering the duration and rate of photosynthesis and respiration of plants, which affects the global vegetation–atmosphere pattern of carbon, water, and energy cycles [6,7]. Among the abiotic factors affecting plant growth, the most immediate and significant influences are temperature and precipitation [8,9]. Climate change can alter temperature and soil moisture levels. Such shifts in hydrothermal conditions can profoundly influence the health and growth of vegetation.

In arid and semi-arid areas, where soil moisture primarily constrains plant growth, a temperature rise elevates evapotranspiration rates, reducing soil water content when temperature and precipitation are negatively and positively correlated with vegetation health, respectively [10]. Considering that spatiotemporal changes in vegetation are closely related to climate change, detecting the spatiotemporal correlation between climate change and vegetation characteristics is important for understanding the impact of climate change on vegetation ecosystems.

Topography, as the most prominent and complex geographical factor in the region, is an important source of environmental spatial and temporal heterogeneity. It influences changes in temperature, precipitation, wind speed, insolation, and evapotranspiration, which are spatially redistributed and can cause local environmental changes, forming microclimate zones and affecting vegetation growth [11]. Topographic factors regulate soil conditions, microclimate, and water availability across regions at small scales [12–14]. As such, they shape the locational conditions for plant growth and drive abiotic and biotic interactions [15], determining plant community diversity, structure, and function [13]. Topography is also important in providing spatial species diversity and expanding ecological niches at different scales, increasing species diversity and resistance to harsh environments [14,16].

More specifically, in the top and slope areas of dunes, nutritious soil and water are often not stored, making the vegetation more competitive for light and nutrients than at the bottom of the dune [13,17]. Currently, the use of variability in topographic features to reveal the spatial distribution patterns of vegetation and the influence of natural factors on vegetation distribution has been widely deployed in the analysis of vegetation patterns at landscape and community scales.

As typical desert vegetation ecosystems, natural oasis regions in the desert hinterlands of China are strongly dependent on water resources. Thus, analyzing the spatial distribution and dynamic changes in vegetation in response to water resources is necessary for the sustainable management and maintenance of healthy ecosystems [18,19]. Relatively abundant and stable water sources in oases provide the necessary water and nutrients for vegetation growth and are prerequisites for the development of natural oases in arid zones [20]. Surface water and its distribution are key factors shaping the spatial vegetation distribution patterns of oases [21].

Groundwater controls vegetation ecosystems [22,23] as a water supply source that supports vegetation growth and transpiration [24,25]. Physiological and ecological indicators of vegetation, water-use strategies, patch distribution characteristics, community abundance, age structure, and succession are closely related to groundwater [26]. Surface water and groundwater jointly influence the survival and development of oasis vegetation. Surface hydrological processes, including the frequency and duration of flooding, determine the distribution pattern of vegetation in riparian zones at the watershed scale, whereas subsurface hydrological processes influence the mechanism between the spatial and temporal ecological succession of natural vegetation, affecting the critical depth of burial of vegetation, ecological water demand of vegetation, and optimum suitable water level for vegetation.

Dramatic climate changes can impact vegetation cover; however, scientific opinions on the drivers of vegetation growth in the Northern Hemisphere are divided. Some researchers posit that global warming is the main cause of increased vegetation cover in the Northern Hemisphere [27]. In contrast, others postulate that global warming increases evaporation and rapidly depletes soil moisture in the arid zones of the Northern Hemisphere, inhibiting

the increase in vegetation cover [28]. Meanwhile, in extremely arid conditions, such as the hinterland of the Taklamakan Desert, although climate change may have an impact, the hydrological processes and topography have an extremely important influence on vegetation cover, significantly affecting the survival and development of vegetation. Within this region, most studies have focused on large-scale assessments, such as the response of vegetation on the Tibetan Plateau to climate change [29] or the impact of climate change on vegetation productivity in the dry zone of Central Asia [30]. Meanwhile, fewer studies have reported small- or medium-scale assessments with regard to changes in vegetation cover.

Located in the desert hinterland, the Daliyabui oasis covers an area of approximately 342 km^2; it represents an area for small- to medium-scale assessments. The use of long-term remotely sensed data is an effective method for studying vegetation changes and atmospheric processes at different spatial and temporal scales [31]. Remotely sensed NDVI calculated from red and near-infrared reflectance has been recognized as an indicator of vegetation cover [32]. Of all the NDVI products, Moderate Resolution (MODIS) NDVI and Landsat NDVI are the most widely used because of their simultaneous high spatial and temporal resolution [33].

Therefore, we selected a natural oasis in the hinterland of the Taklamakan Desert as our research object, with the desert riparian vegetation ecosystem as the core, and explored the effects of climate change, topography, and water resource changes on the spatiotemporal distribution patterns of oasis vegetation. Additionally, we identified the general patterns in desert vegetation characteristics, provided basic datasets for restoring riparian vegetation and curbing oasis desertification, and provided scientific support for oasis health management and sustainable development.

2. Materials and Methods

2.1. Study Area

Nestled within the heart of the Taklamakan Desert—China's grandest desert—lies the Daliyabui oasis, with the borders of 81°90′15″–82°23′41″E and 37°20′39″–39°10′35″N. The core area of the oasis covers an area of 324 km^2, with a relatively flat topography (1061–1177 m) and an average elevation of 1108 m above sea level. The Kriya River traverses this area, flowing from south to north, vanishing into the desert's deep interiors. The oasis predominantly sits on the alluvial plain formed by the tail end of the Kriya River, from which it emerged, presenting a relatively untouched natural sanctuary (Figure 1). The area has a temperate continental arid desert climate characterized by high evaporation, low rainfall, a large diurnal temperature difference, and a long frost-free period. The average annual precipitation is <10 mm, and the average annual temperature is 11 °C. The oasis vegetation composition is dominated by poplars, tamarisks, and reeds, which are representative of the desert ecosystem. Oasis vegetation is mostly distributed in lowlands with shallow groundwater. Poplars primarily grow on both sides of the fine river network, washed out by rivers, shrubs, and annual herbs sparsely growing on sand dunes. In some large inter-mound basins in the interior of the desert, shrubs dominate the plant community, forming relatively large vegetation patches with low coverage.

2.2. Methods

2.2.1. Meteorological and Topographic Data

The impact of climate change on vegetation trends was analyzed using precipitation and temperature data from 2000 to 2020. Ground-based observations were not used in this study as no meteorological stations provided long-term observations in the study area. Therefore, a high-precision 1 km resolution precipitation and temperature dataset was selected and generated for the study area using delta spatial downscaling (http://data.tpdc.ac.cn, accessed on 23 April 2023). Data from 496 independent meteorological observation points were used for validation (Figure 2). Correlation analysis between multi-year meteorological data and NDVI data was performed using Matlab (2021b) software to derive the effect of meteorological factors on vegetation.

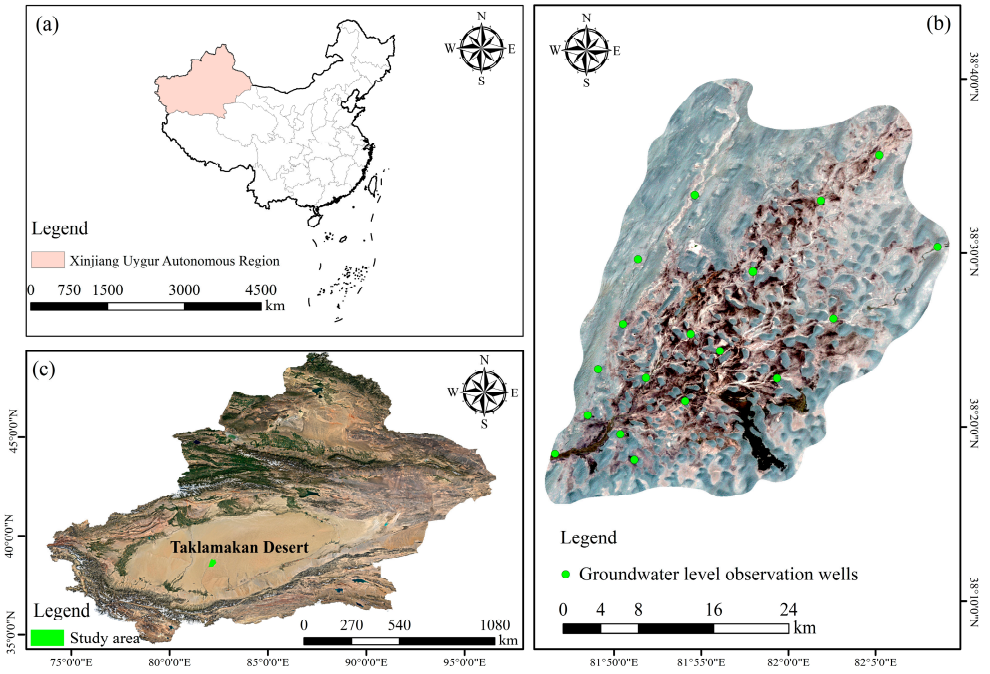

Figure 1. (**a**) Location of study area in China. (**b**) Desert hinterland oasis and ecological water level observation wells. (**c**) Location of the Taklamakan Desert within Xinjiang.

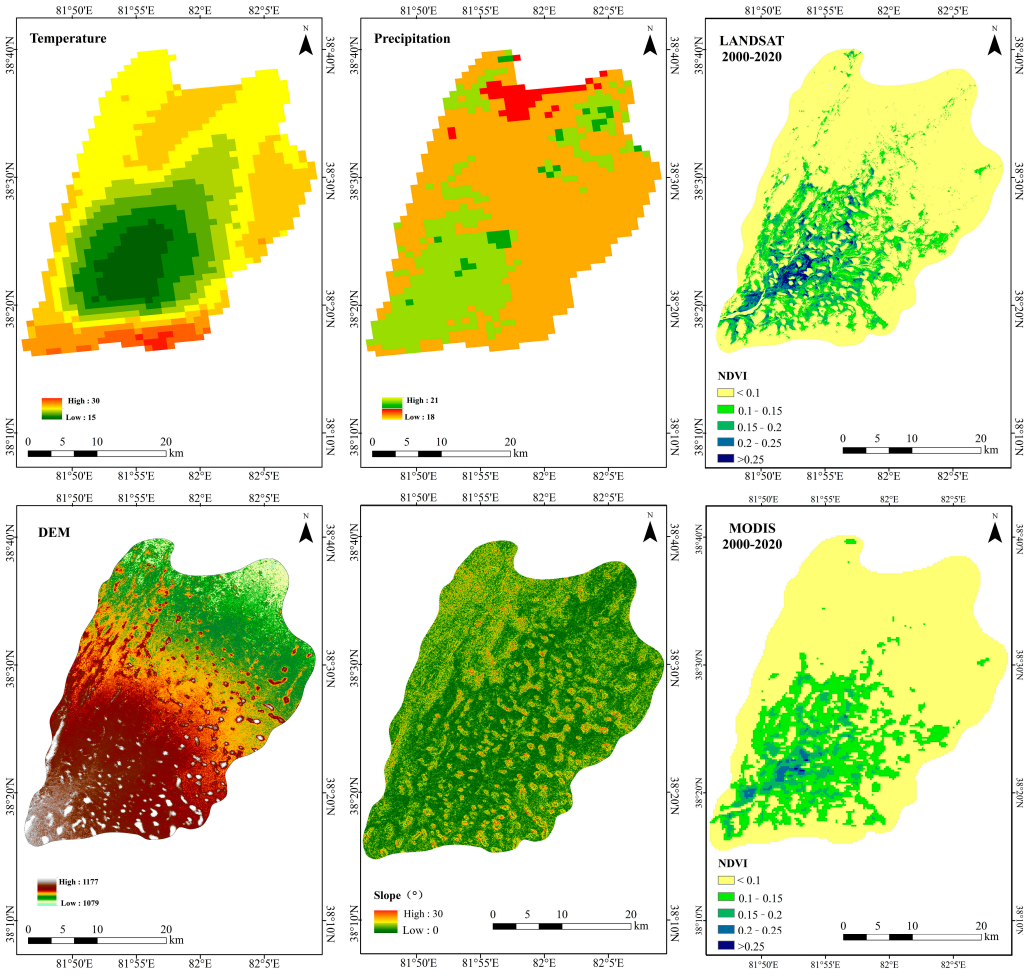

Figure 2. Temperature, rainfall, elevation, slope, and vegetation data for the study area.

To understand the response of vegetation distribution patterns to topography, the 90 m resolution digital elevation model data were used to generate topographic data, calculate and correlate the slope of the study area with vegetation indices, and derive the factors influencing the growth of vegetation (Figure 2). The topographic data were obtained from the U.S. Geological Survey (USGS, https://earthexplorer.usgs.gov/, accessed on 23 April 2023).

2.2.2. Hydrological Data

Surface Water Data

The United States Geological Survey (USGS) provided 130 cloud-free Landsat images from 2000 through 2020 for this investigation. The data were preprocessed using ENVI 5.3 to obtain better-quality images. Then, 13 water body indices were selected to extract water bodies in the study area. This selection considered the degree of numerical differentiation between the surface water image elements and background image elements, that is, the numerical size difference, and the larger the difference, the more conducive it is to the application of automatic thresholding to determine the method of extracting the distribution range of the water bodies and obtaining a better accuracy. Based on a previous analysis [21], the $AEWI_{no\ shadow}$ water body index is the most effective. Mapping the spatial distribution of the surface water was achieved using the maximum entropy threshold segmentation method (Figure 3). Finally, the relative distribution frequency of surface water was obtained by using the TOTAL function to sum the images at the image element scale and dividing by the number of images, N, to normalize the image element values between 0 and 1; 0 indicated that no surface water reached the image element during the study period, and 1 indicated that surface water was always present during the study period. It should be noted that due to image availability and the influence of clouds and cloud shadows, the resulting surface water frequency does not absolutely indicate the presence or absence of surface water, which is in flux, and is only used to characterize the differences in the spatial and temporal distributions of surface water as continuous data for surface water are not available.

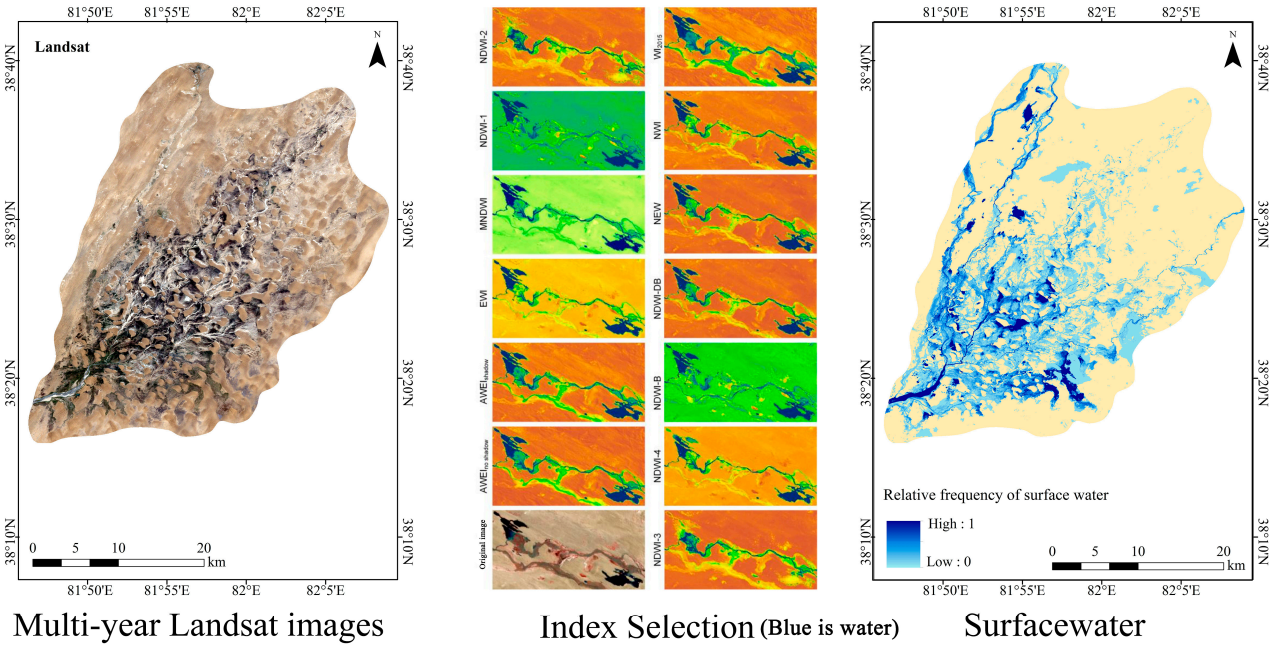

Figure 3. Extraction of surface water processes from remote sensing imagery.

Groundwater Data

To invert the groundwater burial depth, data from 19 groundwater level observation wells (HOBO water level observation meters) in the study area were used to build a model by combining 16 environmental covariates (Figure 4) with high correlation with

groundwater (topographic, meteorological, and vegetation data), and the spatial resolution of the environmental covariates was uniformly re-sampled to 90 m using ArcGIS 10.8. Finally, a groundwater level model was created with Matlab (2021b) software based on the random forest (RF) model, and a remote sensing inversion of the groundwater level in the research region was carried out and mapped.

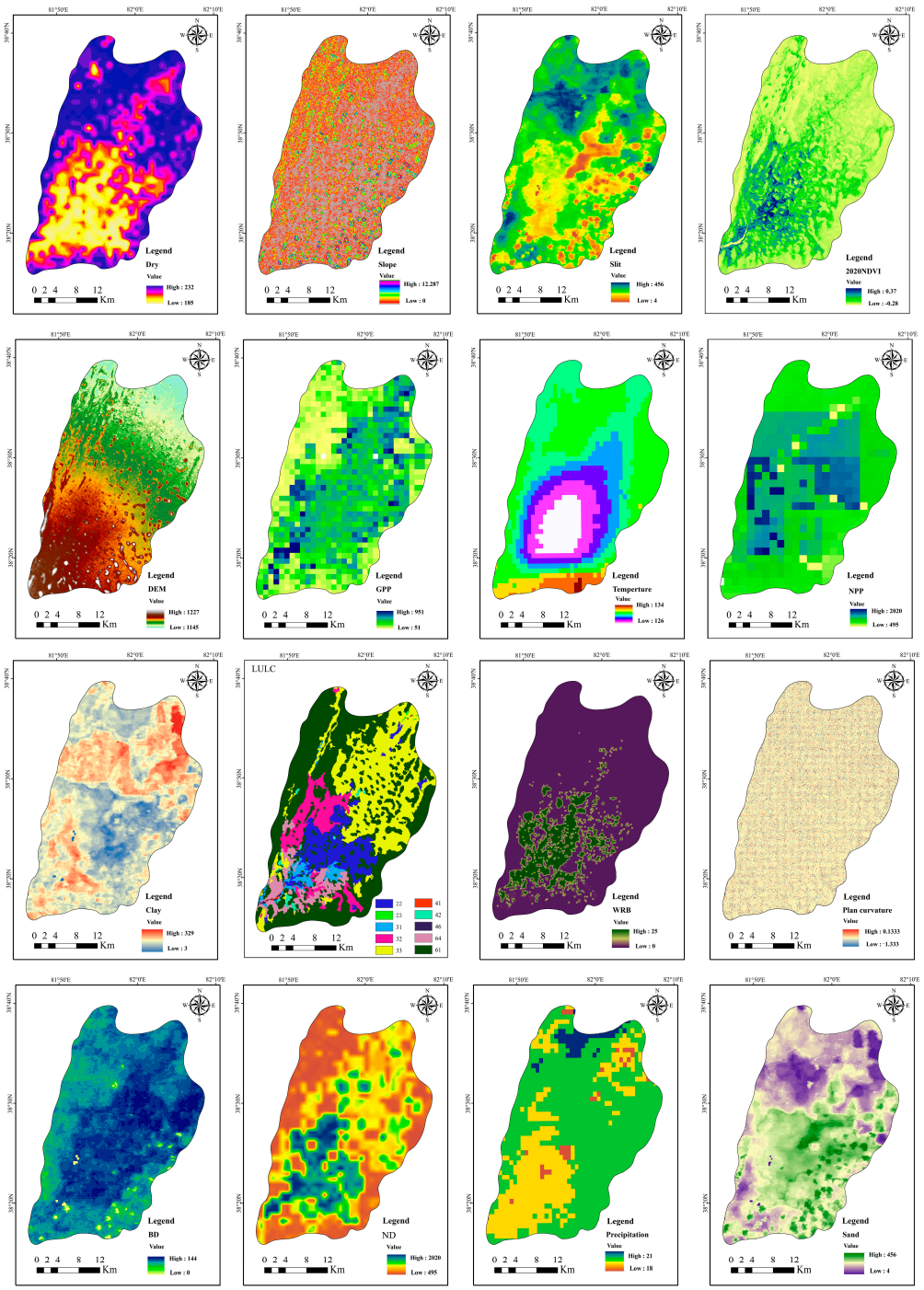

Figure 4. Environmental covariates used for modeling the spatial patterns of groundwater parameters in the Daliyabui oasis (In LULC, 22, 23, 31, 32, 33, 41, 42, 46, 64, 61 represent shrubwood, sparse shrub, high cover grassland, medium cover grassland, low cover grassland, graff, lake, bottomland, marsh, bare land respectively).

To validate the model's ability to predict groundwater burial depth data, we split the entire sample into two. One copy contained samples 9/10 for modeling and 1/10 for validation, yielding ten groups for cross-validation. The model's validity was assessed using root-mean-square error (RMSE) and the coefficient of determination (R^2). The temporal and geographical predictive capacity of the RF model for groundwater parameters may be completely assessed by combining the validation technique for time-varying prediction of the RF model with 10-fold cross-validation (Figure 5).

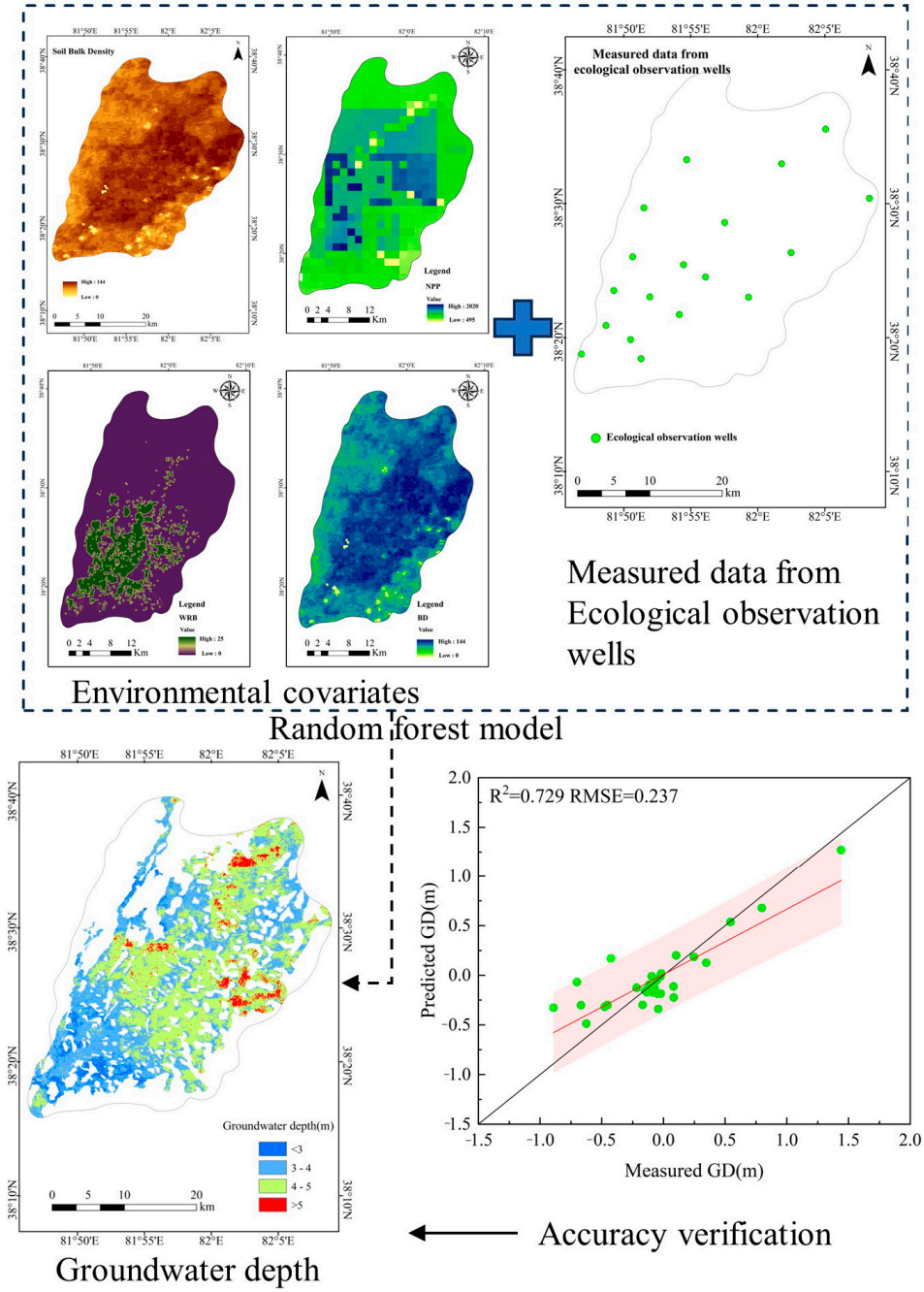

Figure 5. Remote sensing extraction process for groundwater (The green dots represent the coordinates of the measured and predicted points; The red area represents the 95% prediction interval).

2.2.3. Vegetation Data

NDVI is a critical measure for tracking changes in plant distribution patterns in a research region. The Google Earth Engine (GEE) platform was used to calculate NDVI for

the Landsat and MODIS (MODIS/006/MOD13A2) datasets (Table 1) with resolutions of 30 m and 250 m, respectively. The NDVI raster images were obtained by masking the vector range of the study area, cropping the monthly NDVI raster images for 2000–2020, and obtaining the annual average NDVI raster images using the mean method. The comparison of the two time series revealed differences in the Landsat and MODIS satellite sensors that led to uncertainties.

Table 1. Landsat and MODIS satellite sensor information.

Satellites Sensors	Year	Resolution (m)	Period (Days)
Landsat-5 MSS, TM	2000–2013	90	16
Landsat-8 OLI	2013–2020	90	16
MODIS	2000–2020	250	16

Statistical analyses of the Landsat and MODIS NDVI image elements were used to obtain the NDVI distribution characteristics for the entire desert, including the frequency distribution of the NDVI and the mean value. Finally, the nonparametric Mann–Kendall test was performed to determine the statistical significance of the trends for each NDVI dataset for each picture element over the observation period. The calculated statistical indicator Z was used to classify the trends as significant increase ($Z > 1.96$, significant at 5%), significant decrease ($Z < -1.96$, significant at 5%), and no significant change.

2.2.4. NDVI Calculation

NDVI is an important monitoring indicator for quantifying changes in plant cover due to climate change, and it is especially sensitive in arid areas with scant vegetation [34]. The formula is presented in Equation (1):

$$NDVI = \frac{\rho_{nir} - \rho_{red}}{\rho_{nir} + \rho_{red}} \quad (1)$$

where ρ_{nir} is for the near-infrared band and ρ_{red} is for the infrared band.

2.2.5. Water Index Calculation

The $AWEI_{no\ shadow}$ can effectively threshold segment water bodies with high accuracy and improved detection at the surface water distribution's boundaries. It is ideal for monitoring complex water environments in desert areas [35] and is calculated using Equation (2):

$$AWEI_{no\ shadow} = 4(\rho_{green} - \rho_{swir1}) - (0.25\rho_{nir} + 0.75\rho_{swir2}) \quad (2)$$

where ρ_{green}, ρ_{swir1}, ρ_{nir}, and ρ_{swir2} are the reflectance values of the green, *swir*1, near-infrared, and *swir*2 bands, respectively.

2.2.6. Mann–Kendall Test and Sen's Slope Estimator—Trend Detection [36]

Sen's *slope* is widely used in ecohydrological climates and is calculated as per Equation (3):

$$slope = \text{Median}\left[(x_j - x_i)/(j - i)\right], \forall j > i \quad (3)$$

where Median [] represents the median value; if the slope is >0, a positive trend is assigned to the vegetation cover; if the slope is <0, a decreasing trend is assigned.

The Mann–Kendall test is a nonparametric statistical test used to detect the significance of changes in trends and is calculated using Equations (4) and (5):

$$S = \sum_{i=l}^{n-1} \sum_{j=i+1}^{n} sgn(x_j - x_i) \quad (4)$$

$$sgn(x_j - x_i) = \begin{cases} 1(x_j - x_i) > 0 \\ 0(x_i - x_i) = 0 \\ -1(x_j + x_i) < 0 \end{cases} \quad (5)$$

The Z test statistic was used to perform the trend test in Equation (6):

$$\boldsymbol{Z} = \begin{cases} \frac{S}{\sqrt{\mathbf{Var}(S)}} & (\boldsymbol{S} > 0) \\ 0 & (\boldsymbol{S} = 0) \\ \frac{S+1}{\mathrm{Var}(S)} & (\boldsymbol{S} < 0) \end{cases}^{+} \quad (6)$$

where n is the length of the sample and x_i and x_j are the data values in time series i and j, respectively. The formula for Var is presented as Equation (7):

$$\mathrm{Var}(\boldsymbol{s}) = \frac{\mathbf{n}(\mathbf{n}-\mathbf{1})(\mathbf{2n}+\mathbf{5})}{\mathbf{18}} \quad (7)$$

2.2.7. Calculation of Correlation Analysis

Correlation analysis of vegetation with precipitation and temperature was performed using Pearson's correlation coefficient as presented in Equation (8):

$$\boldsymbol{R} = \frac{\boldsymbol{Cov}(\boldsymbol{x},\boldsymbol{y})}{\boldsymbol{\sigma_x \sigma_y}} = \frac{\boldsymbol{n}\sum \boldsymbol{xy} - \sum \boldsymbol{x}\sum \boldsymbol{y}}{\sqrt{\left[\boldsymbol{n}\sum \boldsymbol{x}^2 - (\sum \boldsymbol{x})^2\right] \cdot \left[\boldsymbol{n}\sum \boldsymbol{y}^2 - (\sum \boldsymbol{y})^2\right]}} \quad (8)$$

where R is the correlation coefficient, Cov is the covariance, and σ is the standard deviation.

2.2.8. Random Forest (RF) Model

RF models [37] utilize integrated learning methods and are nonlinear tree-based models. These models use multiple decision trees, making them less prone to oversaturation. Their accuracy is also improved due to the voting of multiple decision trees. Moreover, when dealing with high-dimensional data, there is no need to select features to obtain the value of each. The parallel computing implemented by the RF algorithm is fast and easy to implement, and the introduction of stochasticity reduces the variance of the model run, making it insensitive to multivariate covariances and improving the computation of data with missing values.

Modeling between groundwater level and environmental covariates was performed using RF models in Matlab2018b. Indeed, RFs have better performance in multivariate inversion and can effectively invert groundwater levels, making the results more reliable.

3. Results

3.1. Vegetation Distribution Pattern

The pixel levels of the multiyear average NDVI of the Daliyabui oasis were calculated based on the Landsat and MODIS (Figure 2) NDVI datasets. Although these datasets differ in spatial resolution, they both display comparable distribution patterns. In general, the NDVI at the oasis inlet in the central region was higher than at the tail of the oasis. Higher-resolution Landsat data showed that several sizable vegetation patches with higher NDVI were also distributed in the inner desert region. According to a field survey, these patches of vegetation in the middle of the desert were mostly distributed on both sides of wider river channels, as well as in large open interdune basins surrounded by large sand dunes.

Based on the MODIS and Landsat NDVI datasets, the frequency distribution of NDVI for each image element in the oasis showed a clear single-peaked distribution with a main peak close to 0.06 (Figure 6). This indicated the predominance of sparsely vegetated active dunes in the oasis. The NDVI showed a positively skewed distribution, with the right

side > 0.15 representing vegetation patches. This indicates that the oasis is dominated by low-coverage vegetation with a very small and scattered area of high-density vegetation. This reflects the effects of hydrological and climatic drought conditions on normal vegetation growth.

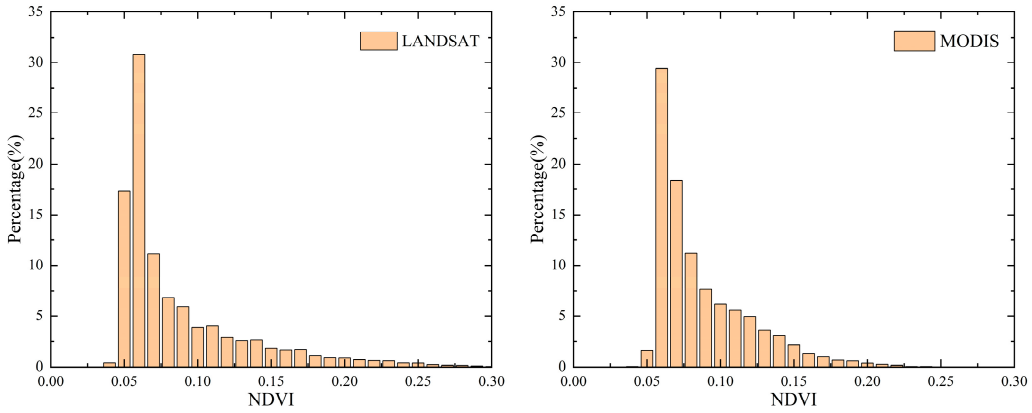

Figure 6. Frequency distribution characteristics of Landsat and MODIS NDVI.

3.2. Greening Trends in the Daliyabui Oasis

The mean values of the Landsat and MODIS NDVI time series were fairly low; both showed a clear rising tendency (Figure 7). The interannual variation in mean NDVI values of both time series was similar, based on Landsat and MODIS NDVI growth rates of 0.001 and 0.0075 per decade during 2000–2020, respectively. Temporally, the oasis vegetation showed an overall greening trend, and degradation existed in local areas. Spatially, the vegetation greening area was primarily distributed in the oasis's western and center areas; the declining area was mainly distributed north of the oasis end and in the eastern region. The stable region was primarily concentrated in the southeastern part of the oasis (Figure 8).

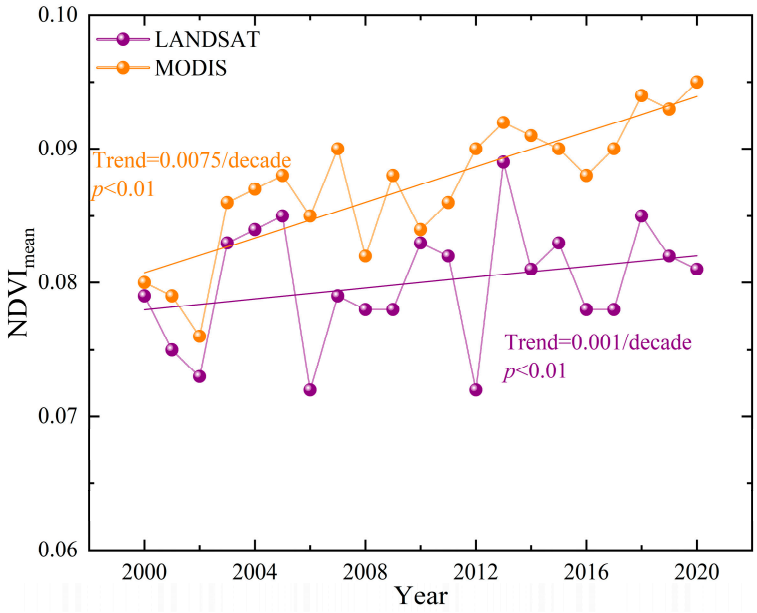

Figure 7. Time series of annual NDVI averages for the entire oasis based on Landsat (purple line) and MODIS (orange line).

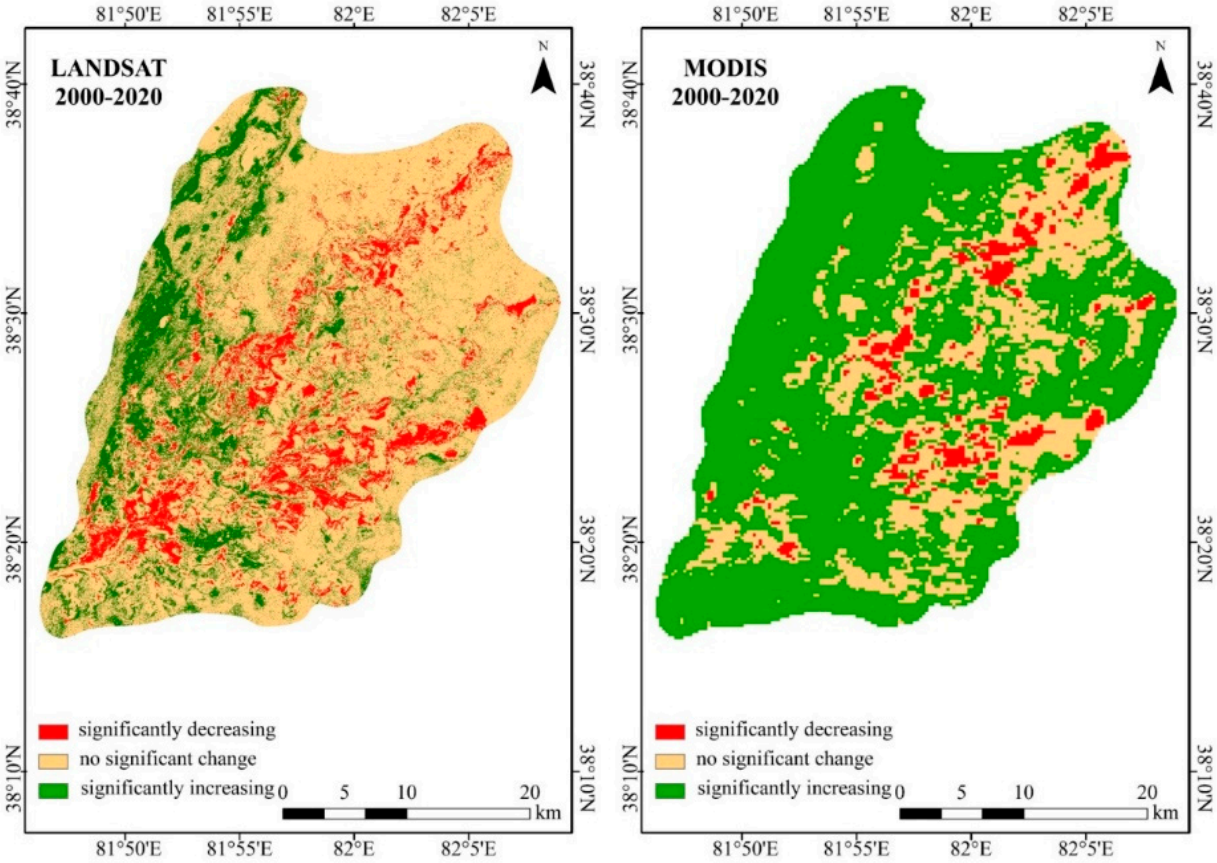

Figure 8. Spatial distribution of annual trends in oasis NDVI.

3.3. Climate Effects of Climate on Oasis Vegetation

Among the various climatic variables that drive vegetation change, the most basic and important are solar radiation, temperature, and precipitation, which provide the light, heat, and water conditions necessary for vegetation growth, respectively [38]. Radiation is the source of energy for plant photosynthesis, which can only proceed under suitable light conditions. Temperature affects the rates of photosynthesis and respiration, as well as the efficiency of nutrient utilization by plants, and precipitation is the main source of plant water [39–41]. Precipitation is thus a key factor for plant growth [42].

Since the 1980s, Northwest China's dry and semi-arid areas have become increasingly warm and humid. The analysis of climatic data showed that the mean and maximum temperatures in the desert hinterland oases increased during the study period (Figure 9a,c). Rainfall showed insignificant interannual variability, while in 2010, there were significant extreme precipitation events (Figure 9b), which had a profound effect on plant growth. At the image metric scale, the relationship between climatic elements such as temperature, precipitation, and NDVI was investigated (Figure 10). The findings revealed that NDVI was positively associated with temperature and precipitation in most of the research locations but was only significant in certain regions ($p < 0.05$). This may be because of the complex response of the NDVI to climate environment changes, which is nonlinear and influenced by topography and hydrological processes [43].

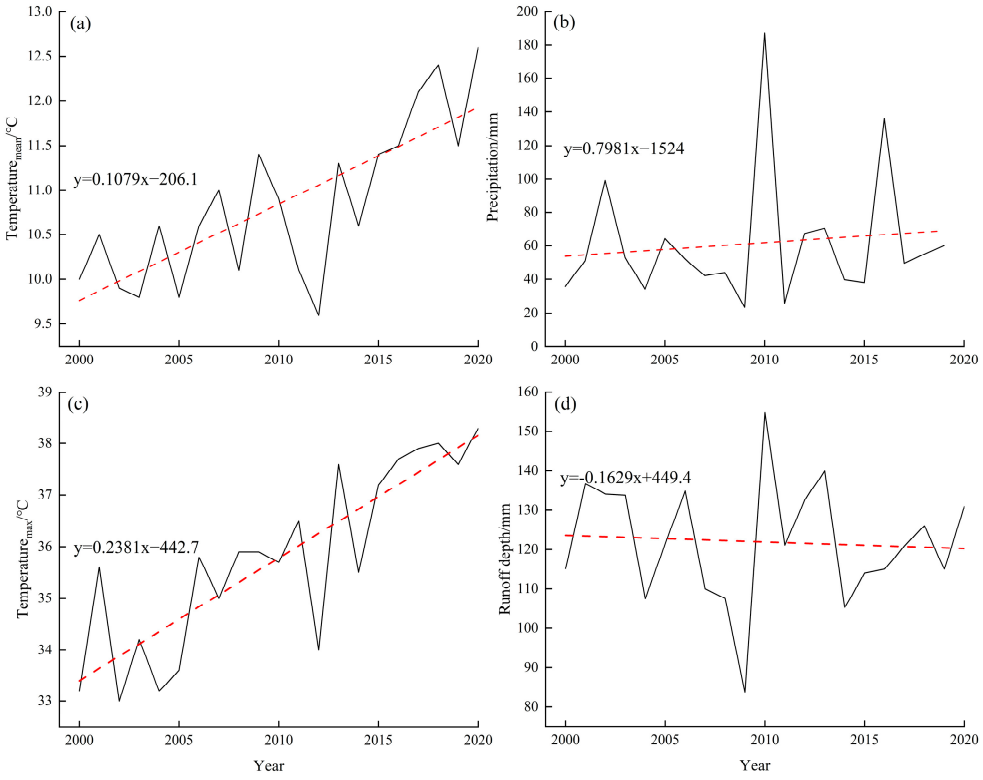

Figure 9. Climatic conditions in the oasis during 2000–2020: (**a**) mean temperature; (**b**) precipitation; (**c**) maximum temperature; (**d**) runoff.

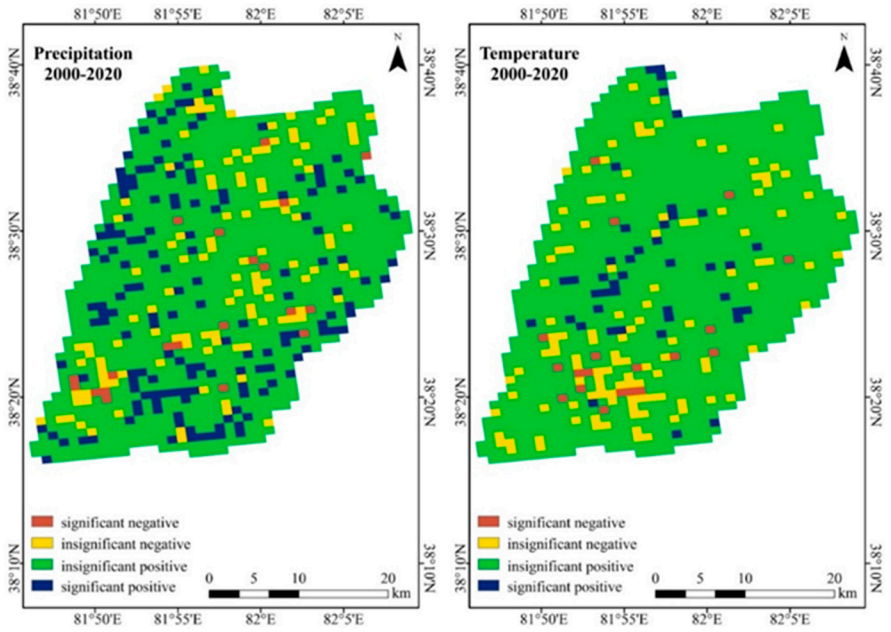

Figure 10. Pearson correlation coefficients between NDVI and precipitation and NDVI and temperature for 2000–2020.

3.4. Effect of Topography on Oasis Vegetation

As shown in Figure 11, regional topography affected the geographic heterogeneity of the observed NDVI distribution. Huge pockets of flora in the hinterland of the desert oasis, which include banded vegetation patches in the middle of the oasis, were typically found in lowlands or vast inter-mound basins with level landscapes, corresponding to the visual interpretation of unmanned aerial vehicle (UAV) images, high-resolution data,

and field surveys (Figure 6). The slopes of the desert hinterland oasis varied greatly in space. (Figure 11). The NDVI pixel values for slopes <8° were larger than those for slopes >8°, where the NDVI was typically below 0.1. Previous research has revealed that local environmental factors regulated by topography impact the development of plants [44].

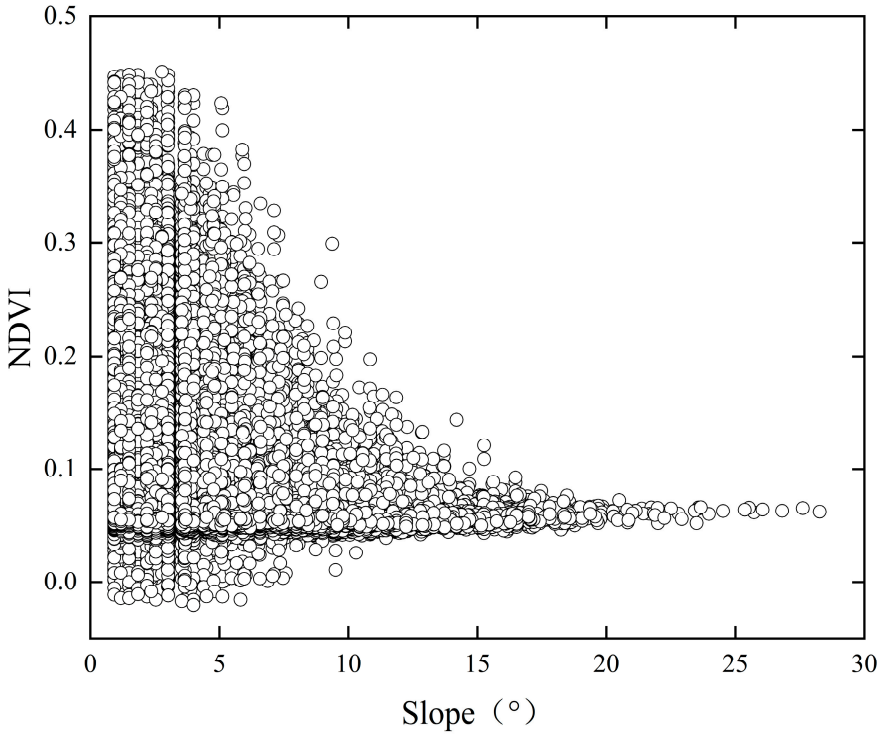

Figure 11. Slope of the study area and NDVI versus slope scatter plot.

Vegetation cover was negatively correlated with slope; that is, the greater the slope, the lower the vegetation cover. The significant variation in vegetation cover with slope is due to the fact that slopes influence surface runoff and water redistribution, creating substantial habitat heterogeneity [45]. Similarly, the size and movement of sand dunes have a significant impact on the geographical distribution pattern of vegetation in desert hinterlands. The geographic spatial distribution pattern of sand dunes affects the distribution and effectiveness of, and accessibility to, surface water, which indirectly affects the spatial distribution of vegetation. Surface water movement has a remodeling effect on sand dunes, driving the transformation of nearby riparian deserts into riverbanks; with the considerable mobility of sand, plants living on dunes are endangered by sand burial.

Meanwhile, in the bottom area of the tall dunes, more water and nutrients can be gathered, providing a good substrate for vegetation growth and development. However, the slope at the top and profile of the dunes prevents water and nutrients from being stored, which is not conducive to the growth of vegetation [46]. Furthermore, the basins formed between individual dunes can provide a more favorable environment for plants to survive in the harsh desert environment by shielding them from wind, sand, and direct sunlight, reducing sand burial and evaporation [47].

3.5. Effects of Spatial Distribution Frequency of Surface Water on Vegetation

Surface water was extracted using the $AEWI_{no\ shadow}$ water body index with the maximum entropy threshold segmentation method from 2000 to 2020. Surface water's relative distribution frequency was obtained by summing all images at the image element scale and dividing by the number (N); this was used to characterize the differences in the spatiotemporal distribution of surface water. The relative distribution frequency of surface water was 1.29. Regarding spatial distribution, the western, central, and southeastern

regions of the oasis were the main distribution areas of surface water; the range was consistent with the vegetation distribution range of the oasis (Figures 7 and 12).

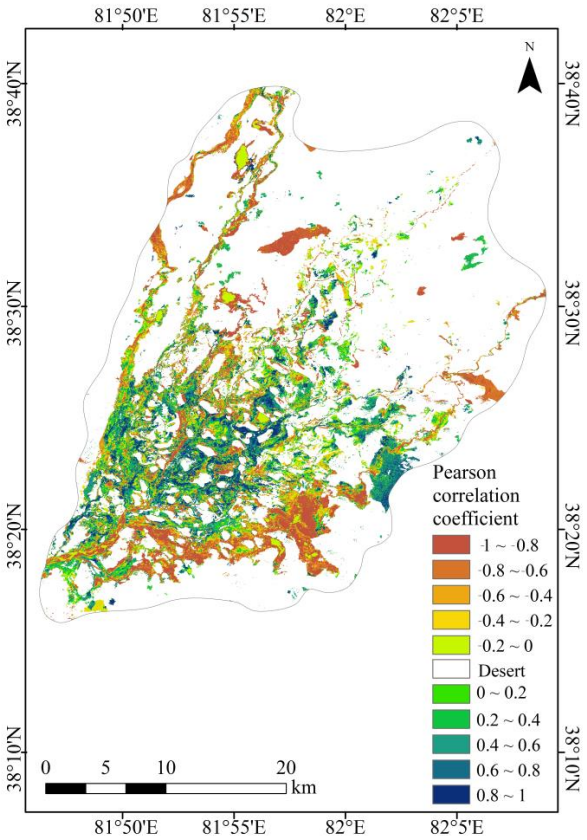

Figure 12. Relative frequency of surface water distribution and correlation with NDVI.

Directionally, 45.54% of the regional surface water frequency in the oasis was positively correlated with NDVI, and 54.46% was negatively correlated with NDVI, owing to the presence of rivers, lakes, waterlogged depressions, and high salinity in high-frequency waterlogged areas (Table 2). Oasis vegetation, water bodies, and sand dunes interact and influence each other, constituting the natural factors controlling changes in the oasis landscape. With the recent change in upstream runoff (Figure 9d), surface water enters the oasis and scours the sand dunes to form the internal river network of the oasis; the accessibility and effectiveness of its water profoundly affect the vegetation on both sides of the river network water system. The surface water end is reduced by the decreased water velocity and flow and the tall sand dunes. This is consistent with the results showing that the topographic slope of the oasis affects vegetation distribution and growth.

Table 2. Frequency correlation of NDVI and surface water distribution from 2000 to 2020.

Classification		Relevance	Percentage	Total
Positive correlation	0.8–1	Very strong positive correlation	8.27%	45.54%
	0.6–0.8	Strong positive correlation	9.41%	
	0.4–0.6	Moderate positive correlation	9.84%	
	0.2–0.4	Weak positive correlation	9.32%	
	0–0.2	Very weak positive correlation	8.70%	
Negative correlation	−0.2–0	Very weak negative correlation	10.20%	54.46%
	−0.4–0.2	Weak negative correlation	8.08%	
	−0.6–0.4	Moderate negative correlation	7.60%	
	−0.8–0.6	Strong negative correlation	11.02%	
	−1–0.8	Very strong negative correlation	17.56%	

3.6. Effect of Groundwater Level on Oasis Vegetation

Groundwater is the main factor influencing plant growth and development [48]. Some studies have concluded that riparian zones are groundwater-sustained ecosystems and that many riparian-zone plants are groundwater-dependent [49]. Groundwater properties (depth of water table burial and groundwater mineralization) determine the distribution of plant composition and diversity in the arid zone [50]. Groundwater can be taken up directly by deep-rooted plants or supplied for the growth of plants with shallow roots as a result of the regulation of the moisture content of the envelope [51]. Changes in groundwater levels can affect water use efficiency and the physiological and ecological responses of plants [52]. To maintain plant growth in riparian zones, the burial depth of the water table must be maintained at a suitable interval. In this study, the burial depth of groundwater in the oasis was mapped based on the environmental covariates selected for correlation with the groundwater level and measured groundwater data. The average depth of groundwater in the vegetated area of the oasis was 3.75 m.

Figure 13 shows that the groundwater burial depth in the vegetated region of the Daliyabui oasis decreased from southwest to northeast, with shallow water table areas at the river inlets on both sides of the oasis, a high groundwater table in the central area owing to topography, and greater groundwater depth in the coccyx area owing to low water accessibility. The groundwater burial depth in the vegetated areas of the oasis ranged from 2 to 7 m, with the minimum and maximum values occurring in small areas in the southern and northern parts of the oasis, respectively. Most of the vegetation was distributed in areas with a groundwater burial depth of 3–5 m, and the distribution range was largest when the groundwater burial depth was 3.5–4.5 m.

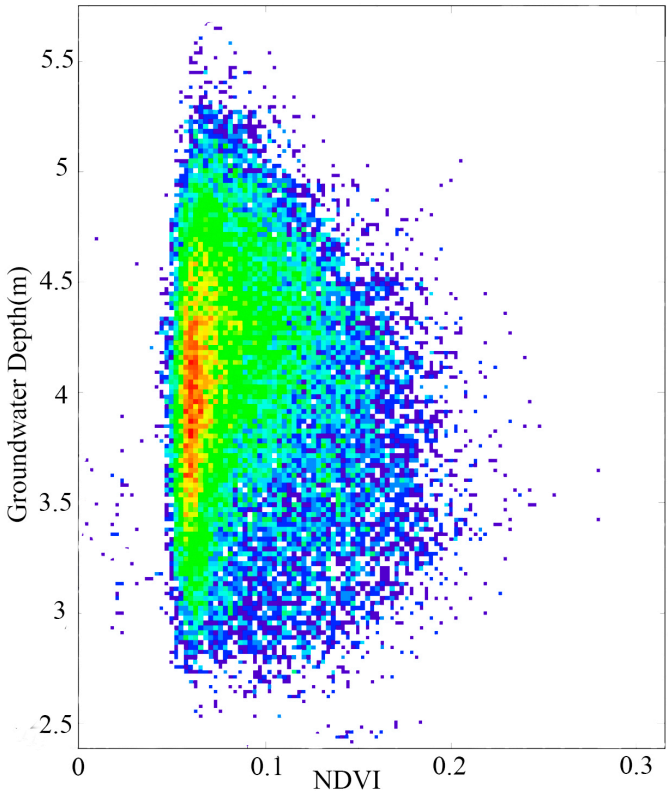

Figure 13. NDVI and groundwater depth scatter plot.

4. Discussion

Arid and semi-arid zones are ecologically fragile, highly sensitive to climate change, and contain vegetation as the main terrestrial ecosystem with vegetation activities producing a dynamic, nonlinear response law that reflects the interaction between hydrothermal

elements and vegetation activities [53]. Although previous studies have provided a preliminary understanding of the increase in vegetation cover change, the results varied widely due to the use of different collection methods, multiple sources of NDVI data, and short NDVI time series [54]. In comparison with Landsat NDVI, LTDR NDVI is more accurate than GIMMS NDVI at the regional scale, in terms of static values and dynamics; however, GIMMS LTDR NDVI data are slightly more accurate than LTDR NDVI data in terms of most vegetation dynamics. This may be due to the GIMMS NDVI values being spatially biased and temporally less biased [55]. Therefore, the use of NDVI data from the same sensor platform and long time series can reduce the data errors caused by different sensor platforms, enabling a better understanding of the changes in vegetation cover in desert hinterland oases and providing a more accurate theoretical basis for predicting changes in vegetation cover and modeling the relationship between vegetation and climate at the global and regional scales. In this study, Landsat, MODIS, and meteorological data did not respond well to the vegetation changes in response to environmental factors due to the limited spatial resolution. However, Sentinel and GF data with higher resolution could be utilized for analysis in subsequent studies. Moreover, this paper only considered the effect of a single environmental factor on vegetation and did not consider the effect of coupling between environmental factors on vegetation. In addition, only climatic, topographic, and hydrological environmental factors were considered, whereas others, such as soil organic matter, nutrient elements, and microclimate, also affect vegetation.

In the present study, 130 Landsat images from 2000 to 2020 were utilized to extract surface water data by adopting the water body index and threshold segmentation method. Although this method achieved better results in water body extraction, the quality and quantity of images and the limitation of spatial and temporal resolution made it difficult for the extracted water bodies to characterize the surface water distribution in the study area accurately. Moreover, only the depth of groundwater burial was modeled using the RF algorithm, with an overall accuracy of 0.729 (Figure 5), indicating that the direct modeling strategy has a limited ability to predict groundwater levels. Zhu et al. improved the prediction accuracy of SPAD using the RF algorithm and a GMM clustering model [56]. Meanwhile, Yang et al. used K-mean and RF machine learning methods, reporting a significant improvement in the accuracy of estimating SPAD [57]. Hence, machine learning methods that are more predictive of groundwater should be introduced in subsequent studies. Moreover, only 16 environmental covariates were included when estimating the depth of groundwater, whereas Zhang et al. selected 24 environmental covariates and used principal component analysis to determine the main variables for predicting soil organic matter in the whole country, which improved the prediction accuracy. Hence, additional environmental covariates should be selected for groundwater level prediction in subsequent studies [37].

5. Conclusions

This study reveals the influence of the distribution pattern of natural oasis vegetation in the hinterland of the Taklamakan Desert by studying the patterns of change in climate, topography, and hydrological processes, and it explores the response of natural oasis vegetation to a series of environmental factors. In general, the oasis vegetation showed a greening trend over time. Spatially, the vegetation showed backward shrinkage in the central region and significant greening in the northwest region. As a result of the effects of climate change, NDVI was positively linked with both temperature and precipitation in the majority of the research locations, but the association was only significant in some parts of the positive correlation region. In natural desert hinterland oases, the most essential element influencing plant growth is water availability, and the combined effects of surface water and groundwater profoundly affect the survival and development of oasis vegetation. A higher frequency of surface water distribution means that the area has better accessibility and water use efficiency, which is also a key factor in shaping the topography of the oasis and determines the distribution pattern of vegetation in the riparian zone at the watershed

scale. The major spatial extent of surface water distribution coincides with vegetation distribution. Meanwhile, a shallow groundwater level affects the mechanism between spatial and temporal ecological succession, critical depth, ecological water demand, and optimal water level of vegetation. Vegetation is most widely distributed in areas with a groundwater burial depth of 3.5–4.5 m. Therefore, this study is informative in exploring how climate change affects oasis vegetation and the impact of water resources on vegetation to guide future water delivery policies for oases.

Author Contributions: Conceptualization and formal analysis, L.P.; funding acquisition, Q.S.; investigation, L.P., Y.W. and H.S.; methodology, L.P.; project administration, Q.S.; software, and A.A.; supervision, Q.S.; validation, L.P., H.S. and A.A.; visualization, L.P.; writing—original draft, L.P.; writing—review and editing, Q.S. All authors have read and agreed to the published version of the manuscript.

Funding: This study was funded by the National Natural Science Foundation of China (Grant No. U1703237).

Data Availability Statement: Data are contained within the article.

Acknowledgments: We are very grateful to our laboratory colleagues for their help in essay writing. We sincerely thank the Editor-in-Chief (Markus Egli) and the two anonymous reviewers for their helpful comments on improving this paper.

Conflicts of Interest: The authors declare no conflict of interest.

References

1. Liang, Y.; Zhang, Z.; Lu, L.; Cui, X.; Qian, J.; Zou, S.; Ma, X. Trend in Satellite-Observed Vegetation Cover and Its Drivers in the Gannan Plateau, Upper Reaches of the Yellow River, from 2000 to 2020. *Remote Sens.* **2022**, *14*, 3849. [CrossRef]
2. Zhang, X.; Jin, X.; Liang, X.; Ren, J.; Han, B.; Liu, J.; Fan, Y.; Zhou, Y. Implications of land sparing and sharing for maintaining regional ecosystem services: An empirical study from a suitable area for agricultural production in China. *Sci. Total Environ.* **2022**, *820*, 153330. [CrossRef] [PubMed]
3. Marques, A.C.; Veras, C.E.; Rodriguez, D.A. Assessment of water policies contributions for sustainable water resources management under climate change scenarios. *J. Hydrol.* **2022**, *608*, 127690. [CrossRef]
4. Alexander, L.V. Global observed long-term changes in temperature and precipitation extremes: A review of progress and limitations in IPCC assessments and beyond. *Weather Clim. Extrem.* **2016**, *11*, 4–16. [CrossRef]
5. Gu, Q.; Wei, J.; Luo, S.; Ma, M.; Tang, X. Potential and environmental control of carbon sequestration in major ecosystems across arid and semi-arid regions in China. *Sci. Total Environ.* **2018**, *645*, 796–805. [CrossRef] [PubMed]
6. Cleland, E.E.; Chiariello, N.R.; Loarie, S.R.; Mooney, H.A.; Field, C.B. Diverse responses of phenology to global changes in a grassland ecosystem. *Proc. Natl. Acad. Sci. USA* **2006**, *103*, 13740–13744. [CrossRef]
7. Piao, S.; Ciais, P.; Friedlingstein, P.; Peylin, P.; Reichstein, M.; Luyssaert, S.; Margolis, H.; Fang, J.; Barr, A.; Chen, A. Net carbon dioxide losses of northern ecosystems in response to autumn warming. *Nature* **2008**, *451*, 49–52. [CrossRef]
8. Nemani, R.R.; Keeling, C.D.; Hashimoto, H.; Jolly, W.M.; Piper, S.C.; Tucker, C.J.; Myneni, R.B.; Running, S.W. Climate-driven increases in global terrestrial net primary production from 1982 to 1999. *Science* **2003**, *300*, 1560–1563. [CrossRef]
9. Wang, H.; Liu, D.; Lin, H.; Montenegro, A.; Zhu, X. NDVI and vegetation phenology dynamics under the influence of sunshine duration on the Tibetan plateau. *Int. J. Climatol.* **2015**, *35*, 687–698. [CrossRef]
10. Yang, L.; Wei, W.; Chen, L.; Chen, W.; Wang, J. Response of temporal variation of soil moisture to vegetation restoration in semi-arid Loess Plateau, China. *Catena* **2014**, *115*, 123–133. [CrossRef]
11. Auslander, M.; Nevo, E.; Inbar, M. The effects of slope orientation on plant growth, developmental instability and susceptibility to herbivores. *J. Arid. Environ.* **2003**, *55*, 405–416. [CrossRef]
12. Ali, A.; Lin, S.-L.; He, J.-K.; Kong, F.-M.; Yu, J.-H.; Jiang, H.-S. Climatic water availability is the main limiting factor of biotic attributes across large-scale elevational gradients in tropical forests. *Sci. Total Environ.* **2019**, *647*, 1211–1221. [CrossRef]
13. Jucker, T.; Bongalov, B.; Burslem, D.F.; Nilus, R.; Dalponte, M.; Lewis, S.L.; Phillips, O.L.; Qie, L.; Coomes, D.A. Topography shapes the structure, composition and function of tropical forest landscapes. *Ecol. Lett.* **2018**, *21*, 989–1000. [CrossRef]
14. Moeslund, J.E.; Arge, L.; Bøcher, P.K.; Dalgaard, T.; Svenning, J.C. Topography as a driver of local terrestrial vascular plant diversity patterns. *Nord. J. Bot.* **2013**, *31*, 129–144. [CrossRef]
15. Stein, A.; Gerstner, K.; Kreft, H. Environmental heterogeneity as a universal driver of species richness across taxa, biomes and spatial scales. *Ecol. Lett.* **2014**, *17*, 866–880. [CrossRef]
16. Lundholm, J.T. Plant species diversity and environmental heterogeneity: Spatial scale and competing hypotheses. *J. Veg. Sci.* **2009**, *20*, 377–391. [CrossRef]
17. Srinivasan, M.P.; Bhatia, S.; Shenoy, K. Vegetation-environment relationships in a South Asian tropical montane grassland ecosystem: Restoration implications. *Trop. Ecol.* **2015**, *56*, 201–217.

18. Gow, L.; Barrett, D.J.; Renzullo, L.J.; Phinn, S.R.; O'Grady, A. A detection problem: Sensitivity and uncertainty analysis of a land surface temperature approach to detecting dynamics of water use by groundwater-dependent vegetation. *Environ. Model. Softw.* **2016**, *85*, 342–355. [CrossRef]
19. Shanafield, M.; Cook, P.G.; Gutiérrez-Jurado, H.; Faux, R.; Eamus, D. Field comparison of methods for estimating groundwater discharge by evaporation and evapotranspiration in an arid-zone playa. *J. Hydrol.* **2015**, *527*, 1073–1083. [CrossRef]
20. Saber, M.; Mokhtar, M.; Bakheit, A.; Elfeky, A.M.; Gameh, M.; Mostafa, A.; Sefelnasr, A.; Kantoush, S.A.; Sumi, T.; Hori, T. An integrated assessment approach for fossil groundwater quality and crop water requirements in the El-Kharga Oasis, Western Desert, Egypt. *J. Hydrol. Reg. Stud.* **2022**, *40*, 101016. [CrossRef]
21. Li, H.; Shi, Q.; Wan, Y.; Shi, H.; Imin, B.; Li, M.S. Influence of Surface Water on Desert Vegetation Expansion at the Landscape Scale: A Case Study of the Daliyabuyi Oasis, Taklamakan Desert. *Sustainability* **2021**, *13*, 9522. [CrossRef]
22. Fan, Y.; Li, H.; Miguez-Macho, G. Global patterns of groundwater table depth. *Science* **2013**, *339*, 940–943. [CrossRef] [PubMed]
23. Shen, C.; Niu, J.; Phanikumar, M.S. Evaluating controls on coupled hydrologic and vegetation dynamics in a humid continental climate watershed using a subsurface-land surface processes model. *Water Resour. Res.* **2013**, *49*, 2552–2572. [CrossRef]
24. Imin, B.; Dai, Y.; Shi, Q.; Guo, Y.; Li, H.; Nijat, M. Responses of two dominant desert plant species to the changes in groundwater depth in hinterland natural oasis, Tarim Basin. *Ecol. Evol.* **2021**, *11*, 9460–9471. [CrossRef] [PubMed]
25. Mcdonald, A.K.; Wilcox, B.P.; Moore, G.W.; Hart, C.R.; Sheng, Z.; Owens, M.K. Tamarix transpiration along a semiarid river has negligible impact on water resources. *Water Resour. Res.* **2015**, *51*, 5117–5127. [CrossRef]
26. Shi, H.; Shi, Q.; Zhou, X.; Imin, B.; Li, H.; Zhang, W.; Kahaer, Y. Effect of the competition mechanism of between co-dominant species on the ecological characteristics of Populus euphratica under a water gradient in a desert oasis. *Glob. Ecol. Conserv.* **2021**, *27*, e01611. [CrossRef]
27. Slayback, D.A.; Pinzon, J.E.; Los, S.O.; Tucker, C.J. Northern hemisphere photosynthetic trends 1982–1999. *Glob. Chang. Biol.* **2003**, *9*, 1–15. [CrossRef]
28. Braswell, B.; Schimel, D.S.; Linder, E.; Moore Iii, B. The response of global terrestrial ecosystems to interannual temperature variability. *Science* **1997**, *278*, 870–873. [CrossRef]
29. Ma, S.; Wang, L.-J.; Jiang, J.; Chu, L.; Zhang, J.-C. Threshold effect of ecosystem services in response to climate change and vegetation coverage change in the Qinghai-Tibet Plateau ecological shelter. *J. Clean. Prod.* **2021**, *318*, 128592. [CrossRef]
30. Wu, L.; Ma, X.; Dou, X.; Zhu, J.; Zhao, C. Impacts of climate change on vegetation phenology and net primary productivity in arid Central Asia. *Sci. Total Environ.* **2021**, *796*, 149055. [CrossRef]
31. Yang, J.; Gong, P.; Fu, R.; Zhang, M.; Chen, J.; Liang, S.; Xu, B.; Shi, J.; Dickinson, R. The role of satellite remote sensing in climate change studies. *Nat. Clim. Chang.* **2013**, *3*, 875–883. [CrossRef]
32. Baniya, B.; Tang, Q.; Huang, Z.; Sun, S.; Techato, K.-a. Spatial and temporal variation of NDVI in response to climate change and the implication for carbon dynamics in Nepal. *Forests* **2018**, *9*, 329. [CrossRef]
33. Beck, P.S.; Atzberger, C.; Høgda, K.A.; Johansen, B.; Skidmore, A.K. Improved monitoring of vegetation dynamics at very high latitudes: A new method using MODIS NDVI. *Remote Sens. Environ.* **2006**, *100*, 321–334. [CrossRef]
34. Jiang, Z.; Huete, A.R.; Chen, J.; Chen, Y.; Li, J.; Yan, G.; Zhang, X. Analysis of NDVI and scaled difference vegetation index retrievals of vegetation fraction. *Remote Sens. Environ.* **2006**, *101*, 366–378. [CrossRef]
35. Fisher, A.; Flood, N.; Danaher, T. Comparing Landsat water index methods for automated water classification in eastern Australia. *Remote Sens. Environ.* **2016**, *175*, 167–182. [CrossRef]
36. Mann, H.B. Nonparametric tests against trend. *Econom. J. Econom. Soc.* **1945**, *13*, 245–259. [CrossRef]
37. Zhang, Z.; Ding, J.; Zhu, C.; Chen, X.; Wang, J.; Han, L.; Ma, X.; Xu, D. Bivariate empirical mode decomposition of the spatial variation in the soil organic matter content: A case study from NW China. *Catena* **2021**, *206*, 105572. [CrossRef]
38. King, D.A.; Bachelet, D.M.; Symstad, A.J.; Ferschweiler, K.; Hobbins, M. Estimation of potential evapotranspiration from extraterrestrial radiation, air temperature and humidity to assess future climate change effects on the vegetation of the Northern Great Plains, USA. *Ecol. Model.* **2015**, *297*, 86–97. [CrossRef]
39. Lenihan, J.M. Climate Cahnge Effects on Vegetation Distribution, Carbon Stocks, and Fire Regimes in California. *AGU Fall Meet. Abstr.* **2002**, *2002*, B21A-0719.
40. Tan, S.Y. The influence of temperature and precipitation climate regimes on vegetation dynamics in the US Great Plains: A satellite bioclimatology case study. *Int. J. Remote Sens.* **2007**, *28*, 4947–4966. [CrossRef]
41. Wang, J.; Price, K.; Rich, P. Spatial patterns of NDVI in response to precipitation and temperature in the central Great Plains. *Int. J. Remote Sens.* **2001**, *22*, 3827–3844. [CrossRef]
42. Chen, H.; Huo, Z.; Dai, X.; Ma, S.; Xu, X.; Huang, G. Impact of agricultural water-saving practices on regional evapotranspiration: The role of groundwater in sustainable agriculture in arid and semi-arid areas. *Agric. For. Meteorol.* **2018**, *263*, 156–168. [CrossRef]
43. Wang, L.; Qiu, Y.; Han, Z.; Xu, C.; Wu, S.-Y.; Wang, Y.; Holmgren, M.; Xu, Z. Climate, topography and anthropogenic effects on desert greening: A 40-year satellite monitoring in the Tengger desert, northern China. *Catena* **2022**, *209*, 105851. [CrossRef]
44. Scherrer, D.; Körner, C. Topographically controlled thermal-habitat differentiation buffers alpine plant diversity against climate warming. *J. Biogeogr.* **2011**, *38*, 406–416. [CrossRef]
45. Bärlocher, F.; Corkum, M. Nutrient enrichment overwhelms diversity effects in leaf decomposition by stream fungi. *Oikos* **2010**, *101*, 247–252. [CrossRef]

46. Chambers, J.C.; Bradley, B.A.; Brown, C.S.; D'Antonio, C.; Germino, M.J.; Grace, J.B.; Hardegree, S.P.; Miller, R.F.; Pyke, D.A. Resilience to stress and disturbance, and resistance to *Bromus tectorum* L. invasion in cold desert shrublands of western North America. *Ecosystems* **2014**, *17*, 360–375. [CrossRef]
47. Akkouche, S.; Guerrache, N.; Bouderbala, R.; Kadik, L. Choice of fixing species dunes and their effect on vegetation. *Int. J.* **2014**, *2*, 21–30.
48. Liu, X.; Lai, Q.; Yin, S.; Bao, Y.; Qing, S.; Mei, L.; Bu, L. Exploring sandy vegetation sensitivities to water storage in China's arid and semi-arid regions. *Ecol. Indic.* **2022**, *136*, 108711. [CrossRef]
49. Balestrini, R.; Delconte, C.; Sacchi, E.; Buffagni, A. Groundwater-dependent ecosystems as transfer vectors of nitrogen from the aquifer to surface waters in agricultural basins: The fontanili of the Po Plain (Italy). *Sci. Total Environ.* **2021**, *753*, 141995. [CrossRef]
50. Xia, J.; Zhang, S.; Zhao, X.; Liu, J.; Chen, Y. Effects of different groundwater depths on the distribution characteristics of soil-Tamarix water contents and salinity under saline mineralization conditions. *Catena* **2016**, *142*, 166–176. [CrossRef]
51. Eamus, D.; Hatton, T.; Cook, P.; Colvin, C. *Ecohydrology: Vegetation Function, Water and Resource Management*; Csiro Publishing: Clayton, Australia, 2006.
52. Antunes, C.; Diaz Barradas, M.C.; Zunzunegui, M.; Vieira, S.; Pereira, Â.; Anjos, A.; Correia, O.; Pereira, M.J.; Máguas, C. Contrasting plant water-use responses to groundwater depth in coastal dune ecosystems. *Funct. Ecol.* **2018**, *32*, 1931–1943. [CrossRef]
53. Zeng, B.; Zhang, F.; Wei, L.; Zhang, X.; Yang, T. An improved IBIS model for simulating NPP dynamics in alpine mountain ecosystems: A case study in the eastern Qilian Mountains, northeastern Tibetan Plateau. *Catena* **2021**, *206*, 105479. [CrossRef]
54. Zhou, J.; Jia, L.; Menenti, M. Reconstruction of global MODIS NDVI time series: Performance of Harmonic Analysis of Time Series (HANTS). *Remote Sens. Environ.* **2015**, *163*, 217–228. [CrossRef]
55. Beck, H.E.; McVicar, T.R.; van Dijk, A.I.; Schellekens, J.; de Jeu, R.A.; Bruijnzeel, L.A. Global evaluation of four AVHRR–NDVI data sets: Intercomparison and assessment against Landsat imagery. *Remote Sens. Environ.* **2011**, *115*, 2547–2563. [CrossRef]
56. Zhu, C.; Ding, J.; Zhang, Z.; Wang, J.; Wang, Z.; Chen, X.; Wang, J. SPAD monitoring of saline vegetation based on Gaussian mixture model and UAV hyperspectral image feature classification. *Comput. Electron. Agric.* **2022**, *200*, 107236. [CrossRef]
57. Yang, X.; Yang, R.; Ye, Y.; Yuan, Z.; Wang, D.; Hua, K. Winter wheat SPAD estimation from UAV hyperspectral data using cluster-regression methods. *Int. J. Appl. Earth Obs. Geoinf.* **2021**, *105*, 102618. [CrossRef]